

Mesoscopic assessment of water droplet collision with a single stainless steel fiber in oil

Bingbing Li^{a,b}, Feng Xin^a, Wei Tan^a, Guorui Zhu^{a,*}

^aSchool of Chemical Engineering and Technology, Tianjin University, Tianjin 300072, China, Tel. +86 22 27408728; Fax: +86 22 27408728; emails: zhuguorui@tju.edu.cn (G. Zhu), libb03@163.com (B. Li), xinf@tju.edu.cn (F. Xin), wtan@tju.edu.cn (W. Tan)

^bDepartment of Chemical Engineering, Renai College of Tianjin University, Tianjin 301636, China

Received 14 October 2018; Accepted 13 June 2019

ABSTRACT

To reveal the flow characteristics in the packed bed of a fiber filter, the collision behaviors of water droplets with a single stainless steel (SS) fiber in oil were investigated. First, the forces acting on the water droplets during collisional processes were analyzed; then, a systematic test based on the visualization method was conducted to elucidate the effects of the emulsion flow rate, the value of $N = r_d/r_f$ (ratio of the radii of the water droplets and the fiber) and oil viscosity on the motions of the water droplets colliding with the fibers. It was revealed that increasing the emulsion flow rate and N can clearly improve the collision velocity and the efficiency of the water droplet collision with a single fiber. However, the influence of the oil viscosity on the velocity of the water droplets approaching the SS fibers can be ignored. All of the findings will facilitate the design of efficient fibrous bed coalescers for emulsion and aerosol purification.

Keywords: Visualization method; Emulsion; Water droplet; Collision; Single fiber

1. Introduction

Water in refinery fuels has received much attention because it gives rise to many problems in the automotive, aviation, and petrochemical industries. Water not only causes corrosion in equipment and engine systems but also influences the lubricative properties of fuel and freezes in subzero conditions, restricting fuel flow and/or damaging the engine system [1–4]. Water is present in fuels in the forms of free water and emulsified water [1,3]. While free water can be separated easily by gravity settling, it is difficult to separate emulsified water from fuels due to the small size (of less than 100 μm) of these water droplets [2,3]. Recently, coalescence filtration has been commonly used to separate emulsified water from oil for economy and efficiency.

However, the performance of fiber filters can be affected by many factors, such as the properties of fluid and emulsion,

the parameters of the fibrous bed, and the operating conditions [5–10]. Many studies have been conducted to examine the effects of the influence factors such as emulsion flow rate, fiber radius, and continuous phase on the fiber filter performance. For example, some researchers have found that the coalescence efficiency of fibrous filters decreased with increasing emulsion flow velocity [11–14], and Li and Gu [15] investigated the effect of the superficial velocity on the filtration efficiency of fiber filter under a lower inlet oil concentration in water, found that the filtration efficiency first increased and then decreased with the increase in the emulsion flow velocity. Additionally, fiber radius also was found to have a clear influence on the filter filtration efficiency. A decrease in the fiber radius can improve the filter filtration efficiency, allowing more small droplets to be removed from the emulsion. Lu et al. [7] and Shin and Chase [16] believed that this improvement was due to the

* Corresponding author.

larger specific surface area and smaller pore size between the fibers. The effects of the continuous phase viscosity on the filtration efficiency of fibrous filter were also studied. Mohammadi et al. [17] and Chiesa et al. [18] demonstrated that the collection efficiency of the fiber filter declined with the increase in the continuous phase viscosity due to the increase in the coalescence time [19].

Although many researchers have studied the effects of various factors on filter performance, their work has mainly focused on the collection efficiency, packed bed pressure drop, and so on. Limited efforts have been devoted to the study of the coalescence mechanisms and flow characteristics involved in the fiber filter packed bed, and these mechanisms have not been understood fully. This may be due to the considerable complexity of the process water droplets undergo during coalescence with the water droplets and fibers in fibrous media [13]. Hence, the complex events occurring in a filter-separator are not adequately understood. The present study aimed to examine the motion of water droplets moving toward and colliding with a single stainless steel (SS) fiber in oil in order to understand the mechanism of fiber filter treatment of water-in-oil emulsion. This research is important for the treatment of water-in-oil emulsions using fibrous filters.

In this paper, first, the forces acting on water droplets during the collisional processes were discussed based on theoretical analysis. Then, a series of experiments were performed by passing a water-in-oil emulsion through a confined cylindrical fiber in a transparent test cell. A visualization method was used to track the motions of water droplets approaching a single microfiber in different experimental conditions. The effects of the emulsion flow rate, the value of $N = r_d/r_f$ and the oil viscosity on the behaviors of the water droplet collision with single SS fibers were also studied in the present work.

2. Theoretical analysis

To better understand the effects of the influence factors on the collisions of water droplets with a single fiber in oil, the forces acting on the water droplets during the collisional processes were analyzed.

The velocity and acceleration of a spherical water droplet i approaching a single fiber can be calculated from the force balance over the droplet.

$$\frac{d\vec{x}_i}{dt} = \vec{v}_i \tag{1}$$

$$m_i \frac{d\vec{v}_i}{dt} = \sum \vec{F}_i \tag{2}$$

In the present work, the effects of the pressure gradient and Basset history force can be neglected due to the microscopic size of the droplets and a small Stokes number [20,21]. Additionally, in this paper, we only focused on the horizontal movements of the water droplets near the fibers; hence, the gravity and buoyancy force were also not considered. The forces $\sum \vec{F}_i$ acting on a spherical water droplet approaching a single fiber have the components of lubrication, drag, and virtual mass (Fig. 1).

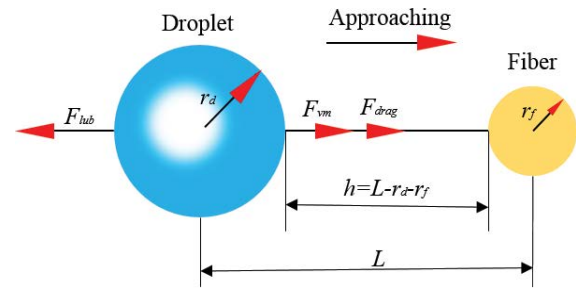


Fig. 1. Radial force components between a water droplet and a single fiber.

$$\sum \vec{F}_i = \vec{F}_{drag} + \vec{F}_{vm} + \vec{F}_{lub} \tag{3}$$

where \vec{F}_{drag} is the drag force from the continuous liquid, \vec{F}_{vm} is the force due to the virtual or added mass effect, and \vec{F}_{lub} is the lubrication force caused by the drainage of the liquid film between the approaching droplets and the fiber.

These forces can be described in greater detail by the following equations [22–25].

$$\vec{F}_{drag} = \frac{1}{2} C_d \rho_c A_d \|\vec{u} - \vec{v}_i\| \times (\vec{u} - \vec{v}_i) \tag{4}$$

$$\vec{F}_{vm} = C_{vm} \rho_c \left(\frac{d\vec{u}}{dt} - \frac{d\vec{v}_i}{dt} \right) \tag{5}$$

$$\vec{F}_{lub} = -\frac{6\pi\mu_c (\vec{v}_i \times \vec{e}_r)}{h} \left(\frac{r_d r_f}{r_d + r_f} \right)^2 \vec{e}_r f^* \tag{6}$$

where in Eqs. (4)–(6), C_d is the drag force coefficient, C_{vm} is the virtual force coefficient, f^* is the lubrication force coefficient, and $h = L - r_d - r_f$ is the gap between the droplet and fiber, as shown in Fig. 1.

In this work, the water droplets can be considered as rigid spheres [20]. This assumption can significantly simplify the calculation of the forces exerted on the water droplets by the oil.

The drag coefficient C_d depends on the Reynolds number based on the total velocity vector. For rigid spheres, the drag force coefficient in Eq. (4) is usually approximated as $C_d \approx 24/Re_d$ [26].

The lubrication force is caused by the drainage of the liquid film between the approaching droplet and the fiber, which is the main force resisting the approach of water droplets to the fiber. For a rigid sphere, $f^* \approx 1$ [20,26].

The virtual mass force generated due to the liquid around water droplet is accelerated by the motion of droplets, which in turn affecting the movement of the water droplets. Following previous studies, the virtual mass force coefficient C_{vm} is considered to have a small constant value of 0.02 [23].

Because only the droplet movements along the horizontal direction are considered, Eqs. (4)–(6) can be transformed as follows:

$$F_{drag} = 6\pi\mu_c r_d (u - v_i)^2 \tag{7}$$

$$F_{vm} = C_{vm} \rho_c \left(\frac{du}{dt} - \frac{dv_i}{dt} \right) \tag{8}$$

$$F_{lub} = -\frac{6\pi\mu_c}{h} \left(\frac{r_d r_f}{r_d + r_f} \right)^2 v_i \tag{9}$$

The ratio of the drag force to the lubrication force can be written as:

$$\left\| \frac{F_{drag}}{F_{lub}} \right\| = \left\| \frac{(u - v_i)^2}{v} \times \frac{h}{r_f} \times \frac{(N + 1)^2}{N} \right\| \tag{10}$$

where N is the ratio of the radii of the water droplet to the fiber, $N = r_d/r_f$.

It is clear from Eqs. (7)–(9) that the influence factors affecting the forces acting on the water droplets are the emulsion flow rate, oil viscosity, and the sizes of the water droplets and the fiber. Therefore, several experiments were performed to study the effects of these factors on the motion of water droplets approaching a single fiber to provide a microscopic understanding of the performance of the fiber filters separating the water droplets from oil.

3. Experiments

3.1. Test cell

The test cell was fabricated by using two polymethyl methacrylate (PMMA) plates (150 mm × 55 mm × 4.5 mm) with a rectangular channel, as shown in Fig. 2a. The channel size was 6 mm (width) × 120 mm (length) × 2 mm (height). The fiber was located in the middle of the channel and was positioned at the midplane to define a symmetric geometry, as shown in Fig. 2b.

3.2. Materials

All of the experiments were carried out at room temperature under atmospheric pressure. Three oil with different viscosities (0[#] diesel oil, 5[#] mineral oil, and 55[#] mineral oil; Sinopec Group, China) were used as the continuous phase, and deionized water was used as the disperse phase. The physical properties of these oils are described in Table 1.

Viscosities of the oil were determined by using a rotating Couette viscometer and the corresponding corrections were taken into account in the analysis of the data. The temperature of the device was determined before and after each set of experiments to ensure that there was no significant temperature variation.

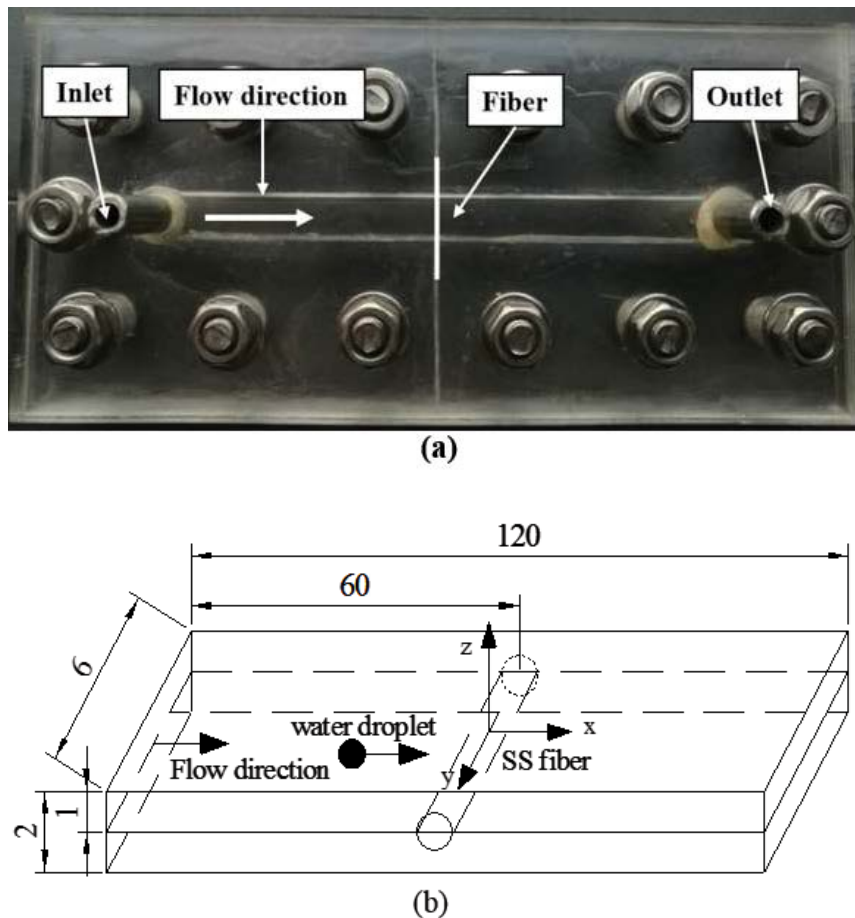


Fig. 2. (a) Photograph of the assembled experimental test cell and (b) structural diagram of the channel and the position of a confined cylindrical fiber.

Table 1
Physical properties of the oil samples (at 20°C)

Property	Density/ ρ_c (g/cm ³)	Viscosity/ μ_c (mPa.s)
0 [#] Diesel oil	0.823	4.65
5 [#] Mineral oil	0.846	7.63
55 [#] Mineral oil	0.876	99.6

Note: All of the values are the average values of three individual measurements.

The fibers used here were 304 stainless steel fibers (SS), and their size was measured with an optical microscope (Olympus CX41; Olympus Corporation, Tokyo, Japan) using Image-Pro Plus. The radii of the SS fibers were 8, 16, 53, and 152 μm , respectively. All of the fibers were thoroughly rinsed with deionized water, acetone, and alcohol and were dried in air overnight.

3.3. Visualization and operation

A diagram of the experimental setup is shown in Fig. 3. The experiments were carried out by using an optical microscope equipped with a high-speed CMOS camera (i-Speed 3, Olympus Corporation, Tokyo, Japan). The images were captured at an exposure time of 200 μs and videos were recorded at 300 frames per second. The water droplet radius r_d was measured from the recorded images. The bulk fluid velocity u and the evolution of the water droplet velocity v_i were both evaluated from the time history of the camera speed and the distance L between the water droplet and the fiber in the recorded videos. The bulk fluid velocity u was acquired according to the microdrop far from the fiber in the upstream, where the influence of fiber on the bulk fluid velocity was negligible. The distance L between the water droplet and the fiber was evaluated for each frame. The local speed of the water droplet was obtained by locating the center of the water droplet in one frame, calculating the relative speed from the movement of the center in several

consecutive frames, and adding the speed of the camera corresponding to these frames. The gap h between the water droplet and the fiber was given by $h = L - r_d - r_f$. The origin of the coordinate system is located on the axis of the fiber as shown in Fig. 2b, so that the value of h is less than 0.

The collision of a single water droplet with a single fiber that we chose to study was approximated to be a head-on collision. This is because in our experiments, we observed that a water droplet of somewhat smaller size, following the streamline that was located at a certain distance from the centerline of the fiber in the flow direction, would pass the fiber without an obvious residence on the surface of fiber, even at the closest approach. However, if the water droplet followed a streamline closer to the centerline of the fiber, the colliding droplets would show a significant residence time on the fiber. Here, we chose to study the water droplets that had a residence time more than 20 ms.

The flow rate of the emulsion through the rectangular channel was controlled by a syringe pump with a 5-mL glass syringe. The emulsion flow rate Q ranged from 0.4 to 2.1 mL/min. After any adjustment of the operating conditions, a time period of at least 30 s was allowed for the stabilization of the system. Several tests were repeated for a single set of operating conditions to provide parallel experiments.

3.4. Emulsion preparation

Water-in-oil emulsions were prepared by mixing oil with 5.0 wt.% deionized water stirred with flat disc saw-tooth disperser (~500 rpm). The sodium alkane sulfonate surfactant (purchased from Tianjin Guangfu Fine Chemical Research Institute, Tianjin, China) in the emulsion was 100 ppm. For better observation of the outline of the water droplets in the emulsion, a water-soluble dye (Acid Red 27, purchased from Tianjin Guangfu Fine Chemical Research Institute, Tianjin, China) was added to the water used in the preparation of the water-in-oil emulsion. The emulsion must be constantly stirred during the experiment to prevent larger water droplets from settling. Fig. 4a shows the image of the emulsion of the water droplet in 55[#] mineral oil that was taken by an

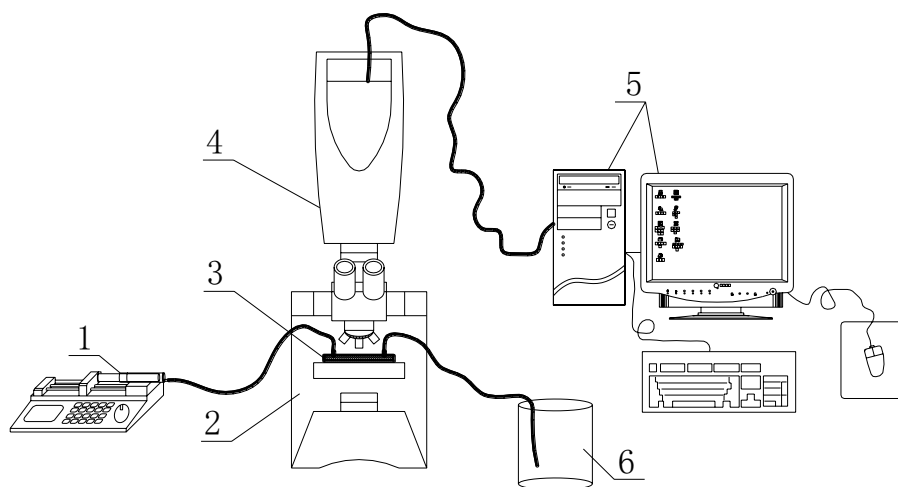


Fig. 3. Schematic of the experimental setup: (1) syringe pump, (2) optical microscope, (3) PMMA test cell, (4) high-speed camera, (5) personal computer, (6) beaker.

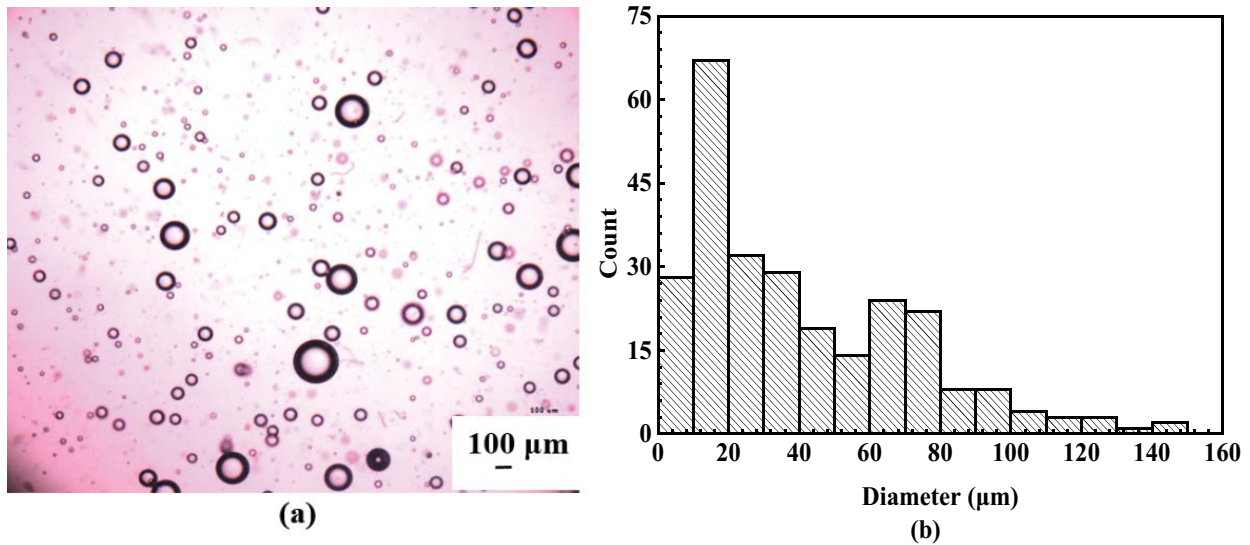


Fig. 4. (a) Emulsion of water droplets in 55# mineral oil and (b) statistics for sizes of the water droplets observed in Fig. 4a.

Olympus CX41 optical microscope, and the droplet diameter distribution is shown in Fig. 4b. The results indicate that most water droplets in emulsion range in size from 20 to 100 μm, and only a small number of water droplets have a diameter larger than 100 μm.

4. Results and discussion

System tests were performed to investigate the effects of three main factors, namely, the emulsion flow rate, the ratio of the radii of the water droplet to the fiber ($N = r_d/r_f$), and the oil viscosity, when evaluating the collision of the water droplet collision with a single fiber in oil. The evolution of the water droplet approach velocity and the number of the water droplet adhering on the fiber were observed to reveal the coalescence mechanism of the fiber filter treating the water-in-oil emulsion.

4.1. Effect of the emulsion flow rate

In this section, the effect of the emulsion flow rate on the water droplet approach velocity and the adhesion of the water droplet on the fiber was investigated. Six different flow rates were studied here, namely $Q = 0.4, 0.6, 0.9, 1.2, 1.5,$ and 2.1 mL/min. The radii of the water droplets and SS fiber used here were $r_d = 20$ and $r_f = 8$ μm, respectively. All of the experiments were performed in 55# mineral oil because the viscosity of 55# mineral oil was sufficiently large, so water droplets were not easily settled from the oil. The velocity of the water droplets approaching the SS fiber and the number of the water droplets adhering on the SS fiber were tracked to reveal the influence of the emulsion flow rate on the performance of a single fiber coalescing with the water droplets.

The evolution of the water droplet approach velocity v_i with the distance h between the droplet and fiber are plotted in Fig. 5a. Comparison of the curves of the water

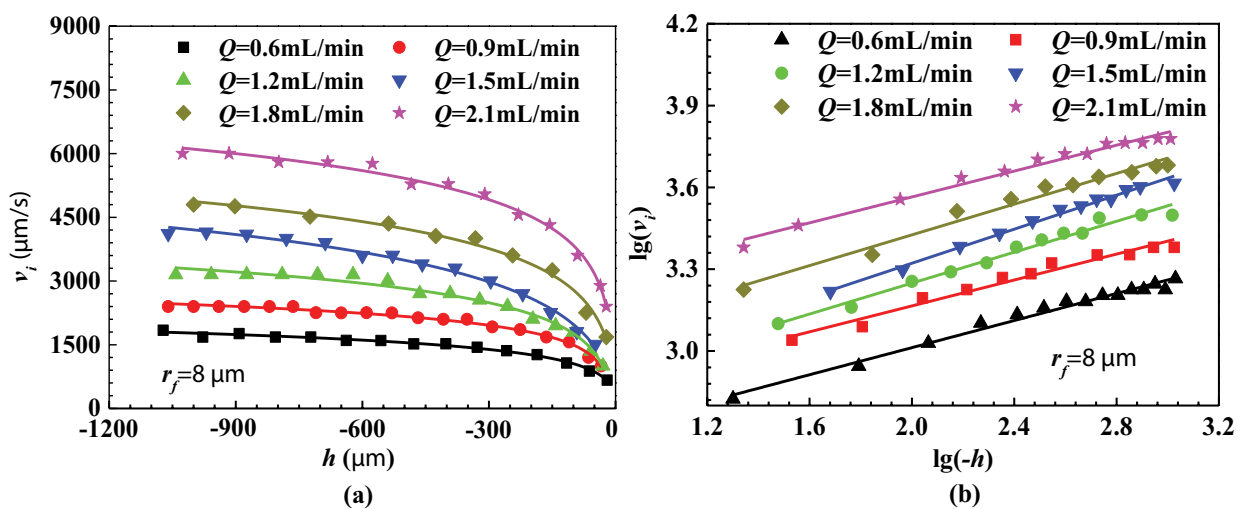


Fig. 5. Effect of the emulsion flow rate (Q) on the evolution of the water droplet approach velocity (v) with the gap between the droplet and the fiber (h). (a) Changes of v_i with h and (b) Log-Log plot of the changes of v_i with $-h$.

droplets approach velocities with h obtained for different emulsion flow rates showed that the emulsion flow rate Q has a clear effect on the approach velocity. A higher emulsion flow rate results in a rapid reduction of the approach velocity, but the approach velocity at the same position is still significantly higher than that for slower emulsion flow rates. For example, as the value of h increases from $-1,000$ to $-50 \mu\text{m}$, that is, as the gap between the water droplet and fiber decreases from $1,000$ to $50 \mu\text{m}$, the water droplet velocity for $Q = 0.6 \text{ mL/min}$ decreases from approximately $1,800$ to $750 \mu\text{m/s}$, corresponding to a decrease of $\sim 63.9\%$; the water drop velocity for $Q = 2.1 \text{ mL/min}$ decreases from approximately $6,100$ to $3,150 \mu\text{m/s}$, decreasing by $\sim 48.4\%$. Moreover, to better compare the velocities of the water droplets near the fiber, the logarithmic variations of the water droplet velocities with $\log(-h)$ are plotted in Fig. 5b. As shown in this figure, the logarithmic variations show a linear relationship, and water droplet logarithmic velocities under a higher emulsion flow rate are clearly larger than those under a lower emulsion flow rate. This behavior is observed because the collision kinetic energy of the water droplet and the drag force acting on the water droplets increase with increasing emulsion flow rate.

Second, the changes in the number and the size of water droplets adhering on the fiber with the changes in the emulsion flow rate were also studied. As shown in Fig. 6, as the emulsion flow rate increases, the number and the size of the water droplets adhering on the fiber first increase and then decrease, with the statistics for the water droplets shown in Table 2. In addition, according to the data presented in the table, as the emulsion flow rate increases from 0.6 to 2.1 mL/min , the number of the water droplet adhering on the fiber reaches the maximum at $Q = 0.9$ and 1.2 mL/min , while the

maximum average radius is observed at $Q = 1.2 \text{ mL/min}$ and is $r_d = 34.6 \mu\text{m}$. This behavior is observed because as the emulsion flow rate increased, the approach velocity of the water droplets increased, which was beneficial for the adhesion of the water droplets on the fiber, but the drag force acting on the sessile water droplets adhering on the fiber also increased. If the emulsion flow rate reached the critical value, the drag force acting on the water droplets can overcome the adhesion force between the droplet and the fiber, and detachment will occur. Hence, the higher flow rate can result in smaller water drops detach from the fiber.

Additionally, in our experiments, we observed that the water droplets with r_d less than $10 \mu\text{m}$ cannot collide with the fiber, as can be confirmed by the sizes of the water droplets adhering on the fiber in Fig. 6, and the motion of the water droplets is significantly affected by the flow field around the fiber, particularly for the small water droplets in the emulsions with a lower flow rate. This is because the collision process of the water droplets on the fiber was determined by the collision kinetic energy. According to Eq. (9), the lubrication force acting on water droplets increases with decreasing gap between the water droplet and the fiber. The water droplets must have sufficient kinetic energy in order to arrive at the fiber surface, and their kinetic energy can be increased by increasing the droplet mass or collision velocity in order to overcome the lubrication force.

As mentioned above, although the droplet collision velocity and the interception efficiency of a single fiber can be enhanced by increasing the emulsion flow rate, the number and the size of the water droplet adhering on the fiber will be decreased if the flow rate is larger than the critical value. Hence, an appropriate choice of the emulsion flow rate is the key to improving the filtration efficiency of the fiber.

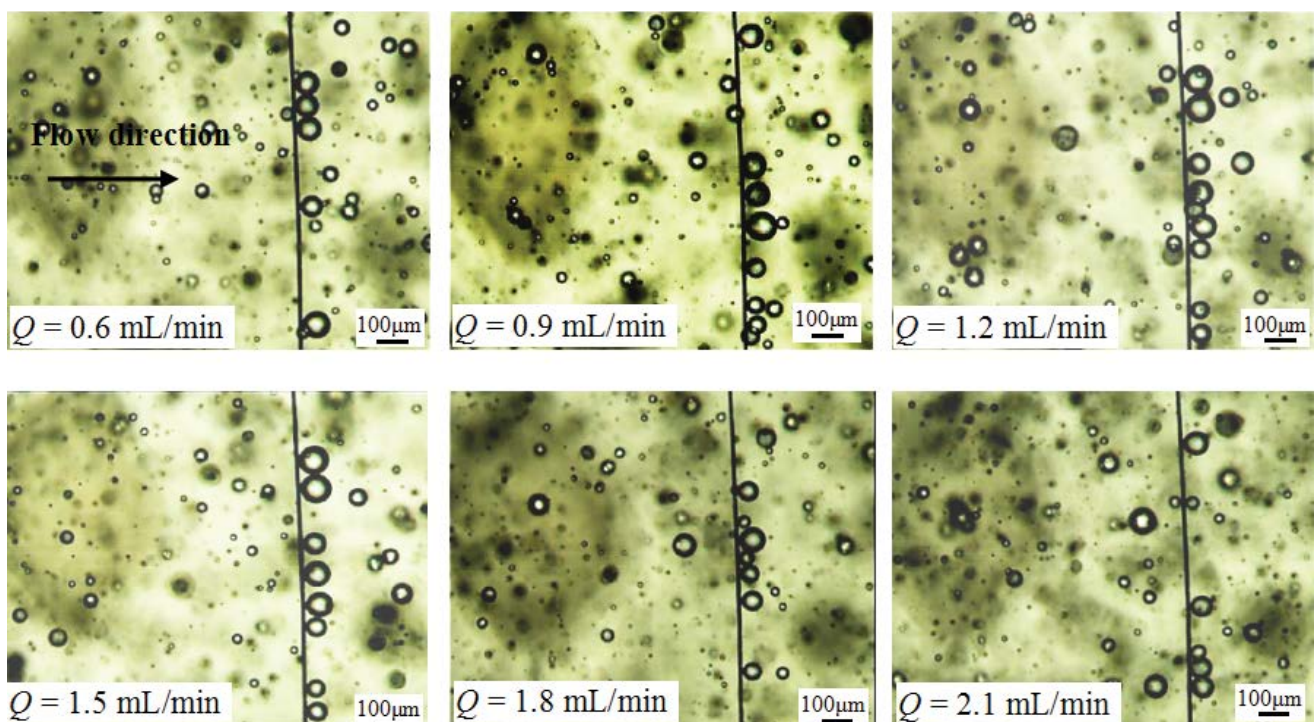


Fig. 6. Photographs of the maximum number of water droplets on the fiber with $r_f = 8 \mu\text{m}$ under different emulsion flow rates.

Table 2
Statistics for the water droplets adhering on the fiber shown in Fig. 6

Flow rate $Q/(mL/min)$	Number of water droplet adhering on the fiber	Radius of the droplets adhering on the fiber/ (μm)		
		Maximum	Minimum	Average
0.6	5	40	28	30.65
0.9	9	44	24	30.8
1.2	9	43	22	34.6
1.5	8	44	18	33.2
1.8	9	40	16	25.3
2.1	6	30	16	25.3

4.2. Effect of the value of $N = r_d/r_f$

The effect of the ratio of the radii the water droplets and the fiber ($N = r_d/r_f$) is discussed here. A series of tests were performed to investigate the effect of N on the motions of the water droplets approaching the fiber and the adhesion of the water droplets on a single fiber in oil. The value of N was varied by changing the radii of either the fiber or the water droplets. All of these tests were performed in 55# mineral oil with an emulsion flow rate of 1.2 mL/min.

In this section, the effect of the fiber radius on the velocities of the water droplets approaching the fiber was studied first. The radii of the fibers used here were $r_f = 8, 53$ and $152 \mu m$, and the radius of the water droplets selected in these tests was approximately $20 \mu m$, corresponding to the values of $N = 0.13, 0.38$, and 2.5 . As shown in Fig. 7a, the effect of N on the water droplet approach velocity is most significant, and a decrease in the value of N (i.e., larger fiber radius) leads to a greater decrease in the water droplet approach velocity. When the value of h increases from -900 to $-60 \mu m$, that is, when the gap between the water droplet and the fiber decreases from 900 to $60 \mu m$, the water droplet approach velocity for $N = 2.5$ decreases from

approximately $3,200$ to $1,600 \mu m/s$; for $N = 0.13$, the water droplet approach velocity decreases from approximately $3,200$ to $600 \mu m/s$, which is approximately 1.6 times that of the value for $N = 2.5$. This behavior is observed because the flow field in the axial section of the fiber was significantly affected by the fiber; thus, increasing the fiber radius can enlarge the area of the flow field that is affected by the fiber, resulting in a decrease in the drag force acting on the water droplets. Moreover, according to Eq. (6), as the fiber radius increases, the lubrication force acting on the water droplet also increases. Hence, increasing the fiber radius, that is, decreasing the value of N , can accelerate the decrease in the water droplet approach velocity.

In addition, the influence of the water droplet radius on the velocity of the water droplets approaching the fiber was also studied. The change in the water droplet size was achieved by carefully selecting a water droplet with a certain radius to be examined based on a large number of experiments. The radii of the water droplets chosen here were $r_d = 36, 42$ and $70 \mu m$, and the fiber radius was fixed at $r_f = 8 \mu m$, corresponding to $N = 4.50, 5.25$ and 8.75 . The results are shown in Fig. 7b. Comparing Fig. 7b with Fig. 7a shows that the variations of the water droplet approach velocities

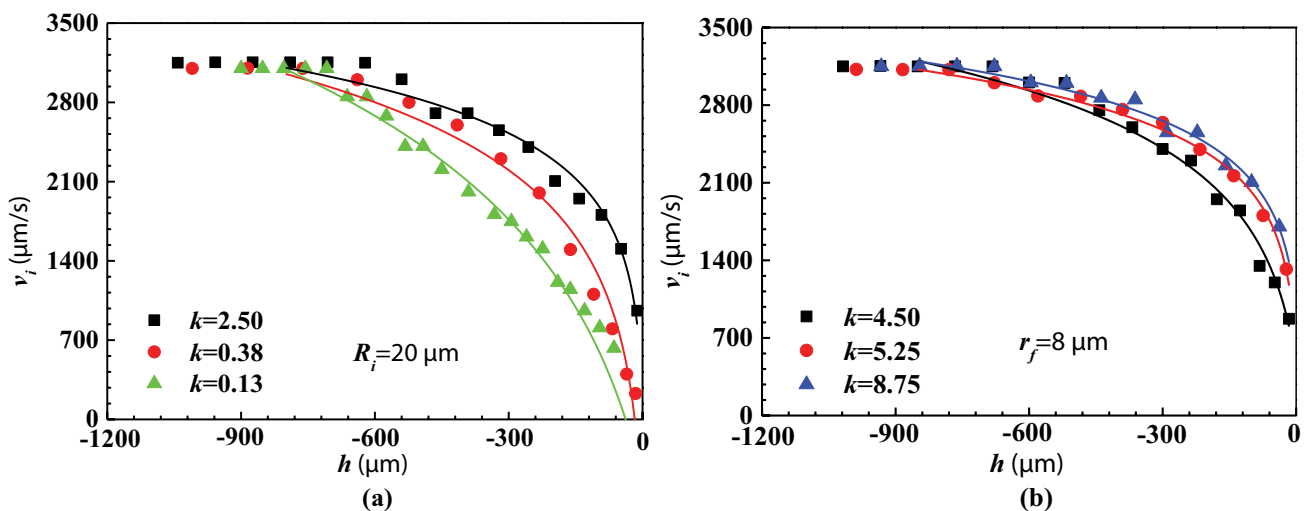


Fig. 7. Effect of the value of N varied by changing either the fiber or water droplet radius, on the evolution of the water droplet approach velocity (v) with the gap between the droplet and fiber (h). (a) Changing the fiber radius and (b) changing the water droplet radius.

with the values of N are similar to those in Fig. 7a; that is, a decrease in the value of N accelerates the decrease in the water droplet approach velocity. This means that larger droplet radius was helpful for the collision of the water droplets with the fiber. According to Eq. (10), it is known that if the fiber radius is fixed, as the value of N increases, the ratio of the drag force to the lubrication force acting on the water droplets also increases. Hence, increasing the radius of the water droplet can also improve the collision of the water droplet and the fiber.

The effect of N on the collision of the water droplets on the fibers can also be confirmed by an examination of Fig. 8. As observed from this figure, the number and the size of water droplets adhering on the smaller fiber ($r_f = 8 \mu\text{m}$) are clearly greater than those on the larger fibers under the same experimental conditions, and the number of the larger water droplet adhering on the fiber is clearly larger than that of the smaller water droplet. Therefore, reducing fiber radius and increasing water droplet radius are effective methods for improving the interception efficiency of the fiber in practical applications.

4.3. Effect of oil viscosity

It is well-known that water separation in heavy crude oil is more difficult than in light crude oil in petroleum dewatering and desalting units due to the higher oil viscosity. To reveal the mechanism by which the oil viscosity affects the motions of the water droplets approaching the fiber, three oils ($0^\#$ diesel oil, $5^\#$ mineral oil, and $55^\#$ mineral oil) with different viscosity values were used to study the effect of the oil viscosity on the process of the water droplets approaching the fiber in this section, and the results are presented in Fig. 9. The radii of fibers used here were $r_f = 8$ and $53 \mu\text{m}$, the size of water droplets selected for study had diameters of approximately $20 \mu\text{m}$, and the emulsion flow rate was 1.2 mL/min .

As shown in Fig. 9, the effect of oil viscosity on the water droplet approach velocity is not obvious. Fig. 9a shows the variations of the water droplet velocities with the value of h/r_f when the fiber radius is $8 \mu\text{m}$ in three different types of oils. As observed from this figure, when the value of h/r_f increases from -120 to -20 , the approach velocity of the water droplet in $55^\#$ mineral oil decreases from approximately $3,100$ to $2,000 \mu\text{m/s}$, decreasing by approximately

$1,100 \mu\text{m/s}$; the approach velocity of the water droplet in $0^\#$ diesel oil decreases from approximately $3,100$ to $1,870 \mu\text{m/s}$, decreasing by approximately $1,230 \mu\text{m/s}$, which is only approximately 1.1 times of that in $55^\#$ mineral oil. Moreover, when the value of h/r_f is larger than -20 , the differences in the water droplet approach velocities in three different oils are much smaller than that of the value of h/r_f between -120 and -20 .

To better understand the effect of oil viscosity on the variations of the water droplets velocities with the h/r_f larger than -20 , the processes of the water droplets approaching a larger fiber with $r_f = 53 \mu\text{m}$ were studied here, and the results are shown in Fig. 9b. Comparing this figure with Fig. 9a shows that the variations of the water droplets approach velocities with h/r_f are similar, and the differences in the water droplets approach velocities in three different oils are very small. In Fig. 9a, when the value of h/r_f holds between -120 and -20 , the relative errors of the water droplets approach velocities are less than 3.8%, while when the value of h/r_f is larger than -20 , the relative errors are smaller than that of the value of h/r_f between -120 and -20 , and the largest relative errors are only about 2.4%, as shown in Fig. 9b.

According to Eqs. (8) and (10), it is known that the virtual mass force and the ratio of drag force to lubrication force are independent of the oil viscosity, but the virtual mass force depends on the density of the oil. When the value of h/r_f is between -120 and -20 , the virtual mass force is not negligible compared with the drag force and the lubrication force; hence, the water droplet approach velocity can be affected by the virtual mass force, even though the effect is very small due to the differences between the densities of the three different oils are small (as shown in Table 2). However, when the value of h/r_f is larger than -20 , the virtual mass force is negligible compared with the drag force and the lubrication force. According to Eq. (2), the accelerations of water droplets of the same radius are the same under the same experimental conditions. Hence, the differences in the water droplets approach velocities between the three oils were very small when the value of h/r_f was larger than -20 .

In addition, in our experiments, we found that the number of the water droplets adhering to the fiber was increased with increasing oil viscosity, as shown in Fig. 10. The main reasons for this behavior were as follows: first, the test cell is placed horizontally in our experiments, and the large water

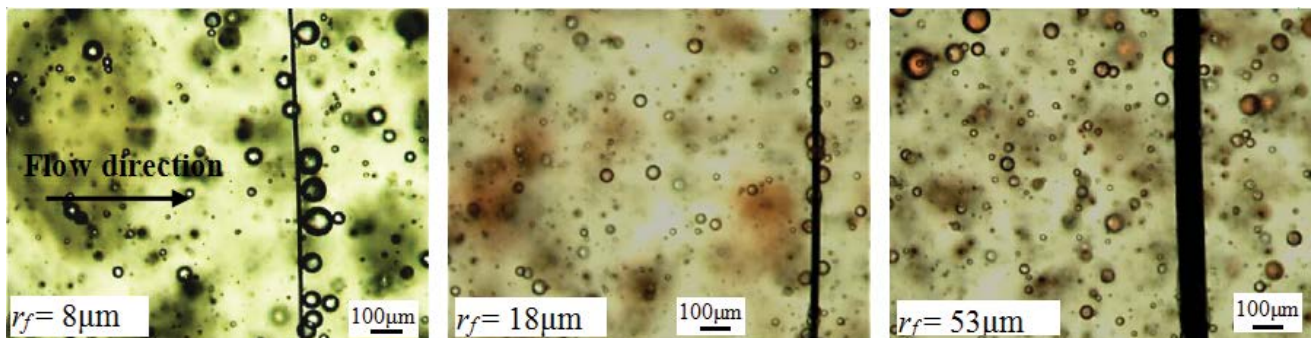


Fig. 8. Photographs of the maximum number of the water droplets adhering on the SS fiber for different droplet radius under the same experimental conditions.

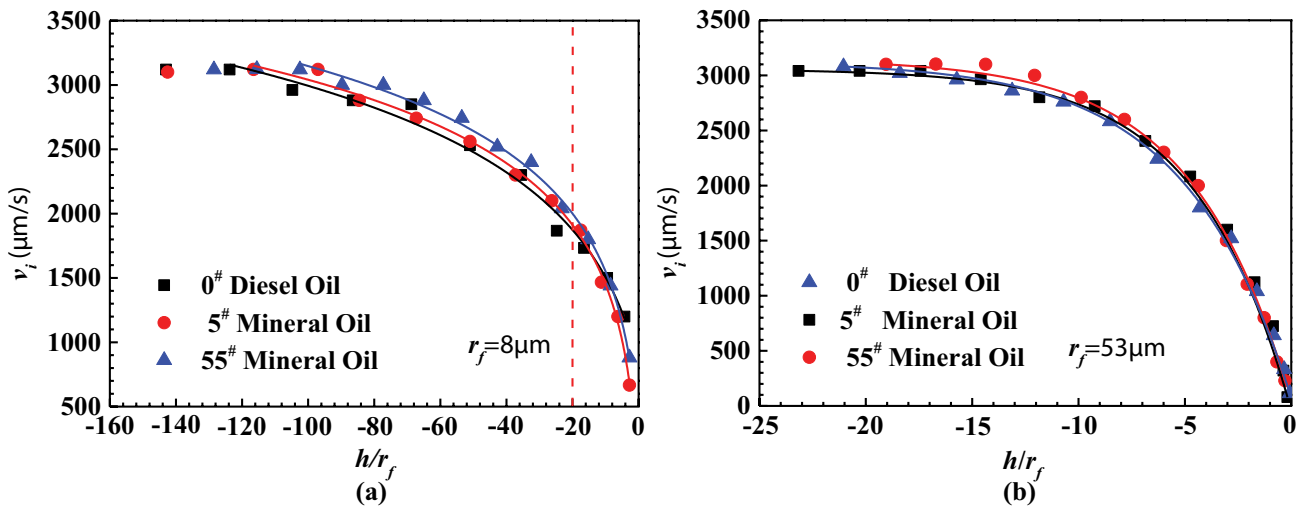


Fig. 9. Effect of oil viscosity on the evolution of water droplet approach velocity (v) with the gap between the droplet and fiber (h). (a) Fiber radius $r_f = 8 \mu\text{m}$ and (b) fiber radius $r_f = 53 \mu\text{m}$.

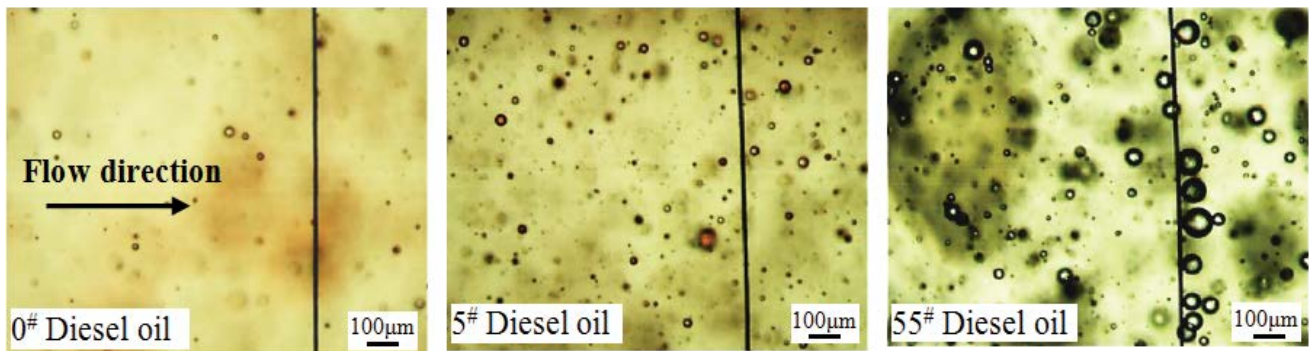


Fig. 10. Photographs of the maximum number of water droplets on the SS fiber with $r_f = 8 \mu\text{m}$ in oils with different viscosities.

droplets can be easily separated from the lower viscosity oil due to gravity; second, according to Eq. (7), as the oil viscosity increased, the drag force acting on water droplets also increased, which was beneficial for the adhesion of the water droplet on the fiber when the water droplets collided and stayed on the fiber surface. Therefore, the number and the size of the water droplets adhering on the fiber increased with increasing oil viscosity under the same experimental conditions.

As mentioned above, for a small water droplet in oil, an increasing oil viscosity is helpful for the collision and the adhesion of the water droplet on the fiber and can improve the fiber interception efficiency of water droplets. This is different from the previous reports that higher oil viscosity decreases the collection efficiency of the fiber filter [19]. This result may be obtained because we only investigated the effect of oil viscosity on the processes of water droplet collision with the fiber, and we did not examine the subsequent processes, such as the release of the enlarged water droplet from fiber surface and the settlement of the water droplets in oil. Each of these steps involves considerable complexity. All of these steps can affect the coalescence efficiency of the fiber filter.

5. Conclusion

In the present work, we sought to understand the coalescence mechanism and the flow characteristics in the fiber filter treatment water-in-oil emulsion by investigating the processes of water droplets approaching and colliding with a single SS fiber in oil. First, the forces acting on the water droplets during the collisional processes with the fiber were analyzed; then, based on the theoretical analysis, the effects of the three main factors on the motions of the water droplet colliding with the fiber were studied. The following conclusions can be drawn from this work:

- Increasing the emulsion flow rate can raise the collision velocities of the water droplets on the fibers, which will improve the interception efficiency and the inertial collision efficiency of single fibers. However, a higher flow rate, in turn, reduced the number and size of the water droplets adhering to the fibers.
- Increasing the value of N can reduce the effect of the fiber on the motion of the water droplets approaching the fiber, which was helpful for the collision of the water droplets with the fiber. However, most of the water

droplets approaching the fiber cannot easily collide with the fiber due to the effect of the flow field around the fiber, with the exception of the water droplets that have sufficient kinetic energy.

- The influence of oil viscosity on the collision processes between the water droplets and the fibers can be ignored.

These results are very useful for better understanding the mechanism of emulsion separation through a fiber filter and determining the optimum operating conditions, but they also suggest several new questions for guiding further studies in this field.

Acknowledgments

This work was supported by Tianjin key research and development program (17YFCZZC00290) and the National Students' Innovation and Entrepreneurship Training Program (201814038004).

Symbols

r_d	— Droplet radius
r_f	— Fiber radius
N	— Ratio of the radii of the water droplet to the fiber ($N = r_d/r_f$)
h	— Least-distance between the water droplet and the fiber
C_d	— Drag coefficient
C_{vm}	— Virtual force coefficient
Re_d	— Droplet Reynolds number ($Re_d = 2\rho_c r_d v / \mu_c$)
\vec{F}_{lub}	— Lubrication force vector
\vec{F}_{vm}	— Virtual mass force
\vec{F}_{drag}	— Drag force vector
f^*	— Lubrication force coefficient
L	— Center distance between the water droplet and the fiber
\vec{u}	— Emulsion phase velocity vector
\vec{v}_i	— Droplet velocity vector
Q	— Emulsion flow rate
x_i	— Droplet position vector
μ_d	— Viscosity of droplet
μ_c	— Viscosity of the continuous phase
ρ_d	— Density of droplet
ρ_c	— Density of the continuous phase
i	— Droplet i
\vec{e}_r	— Relative motion vector

References

- [1] R.L. Brown, T.H. Wines, Improve suspended water removal from fuels, *Hydrocarbon Process.*, 72 (1993) 95–100.
- [2] P.S. Kulkarni, S.U. Patel, G.G. Chase, Layered hydrophilic/hydrophobic fiber media for water-in-oil coalescence, *Sep. Purif. Technol.*, 85 (2012) 157–164.
- [3] S.K. Prashant, Mixed Hydrophilic/Hydrophobic Fiber Media for Liquid-Liquid Coalescence, The University of Akron, Ann Arbor, 2011.
- [4] Y. Li, J. Schnable, Solving water contamination problems in lubrication oil, *Filtr. Sep.*, 37 (2000) 18–21.
- [5] B.J. Mullins, I.E. Agranovski, R.D. Braddock, C.M. Ho, Effect of fiber orientation on fiber wetting processes, *J. Colloid Interface Sci.*, 269 (2004) 449–458.
- [6] S. Agarwal, V. von Arnim, T. Stegmaier, H. Planck, A. Agarwal, Effect of fibrous coalescer geometry and operating conditions on emulsion separation, *Ind. Eng. Chem. Res.*, 52 (2013) 13164–13170.
- [7] H. Lu, Q. Yang, S. Liu, L.-S. Xie, H.-I. Wang, Effect of fibrous coalescer redispersion on W/O emulsion separation, *Sep. Purif. Technol.*, 159 (2016) 50–56.
- [8] R.M.Š. Sokolovic, T.J. Vulic, S.M. Sokolovic, Effect of fluid flow orientation on the coalescence of oil droplets in steady-state bed coalescers, *Ind. Eng. Chem. Res.*, 45 (2006) 3891–3895.
- [9] R.M.Š. Sokolovic, S.M. Sokolovic, and B.D. Đokovic, Effect of working conditions on bed coalescence of an oil-in-water emulsion using a polyurethane foam bed, *Ind. Eng. Chem. Res.*, 36 (1997) 4949–4953.
- [10] M.M. Amrei, M. Davoudi, G.G. Chase, H.V. Tafreshi, Effects of roughness on droplet apparent contact angles on a fiber, *Sep. Purif. Technol.*, 180 (2017) 107–113.
- [11] D.F. Sherony, R.C. Kintner, Coalescence of an emulsion in a fibrous bed: Part II. Experimental, *Can. J. Chem. Eng.*, 49 (1971) 321–325.
- [12] R.N. Hazlett, Fibrous bed coalescence of water. role of a sulfonate surfactant in the coalescence process, *Ind. Eng. Chem. Fundam.*, 8 (1969) 633–640.
- [13] R.N. Hazlett, Fibrous bed coalescence of water. Steps in the coalescence process, *Ind. Eng. Chem. Fundam.*, 8 (1969) 625–632.
- [14] Y. Liao, D. Lucas, A literature review on mechanisms and models for the coalescence process of fluid particles, *Chem. Eng. Sci.*, 65 (2010) 2851–2864.
- [15] J. Li, Y. Gu, Coalescence of oil-in-water emulsions in fibrous and granular beds, *Sep. Purif. Technol.*, 42 (2005) 1–13.
- [16] C. Shin, G.G. Chase, Water-in-oil coalescence in micro-nanofiber composite filters, *AIChE J.*, 50 (2004) 343–350.
- [17] M. Mohammadi, S. Shahhosseini, M. Bayat, Direct numerical simulation of water droplet coalescence in the oil, *Int. J. Heat Fluid Flow*, 36 (2012) 58–71.
- [18] M. Chiesa, S. Ingebrigtsen, J.A. Melheim, P.V. Hemmingsen, E.B. Hansen, Ø. Hestad, Investigation of the role of viscosity on electrocoalescence of water droplets in oil, *Sep. Purif. Technol.*, 50 (2006) 267–277.
- [19] A.K.A. Chesters, The modelling of coalescence processes in fluid-liquid dispersions: a review of current understanding, *Chem. Eng. Res. Des.*, 69 (1991) 259–270.
- [20] M. Chiesa, J.A. Melheim, A. Pedersen, S. Ingebrigtsen, G. Berg, Forces acting on water droplets falling in oil under the influence of an electric field: numerical predictions versus experimental observations, *Eur. J. Mech. B. Fluids*, 24 (2005) 717–732.
- [21] E.E. Michaelides, Hydrodynamic force and heat/mass transfer from particles, bubbles, and drops—the Freeman scholar lecture, *J. Fluids Eng.-Trans. ASME*, 125 (2003) 209–238.
- [22] S. Laín, D. Bröder, M. Sommerfeld, M.F. Göz, Modelling hydrodynamics and turbulence in a bubble column using the Euler-Lagrange procedure, *Int. J. Multiphase Flow*, 28 (2002) 1381–1407.
- [23] Z. Shang, J. Lou, H. Li, A novel Lagrangian algebraic slip mixture model for two-phase flow in horizontal pipe, *Chem. Eng. Sci.*, 102 (2013) 315–323.
- [24] G.H. Yeoh, J. Tu, Numerical modelling of bubbly flows with and without heat and mass transfer, *Appl. Math. Modell.*, 30 (2006) 1067–1095.
- [25] L.X. Zhou, M. Yang, C.Y. Lian, L.S. Fan, D.J. Lee, On the second-order moment turbulence model for simulating a bubble column, *Chem. Eng. Sci.*, 57 (2002) 3269–3281.
- [26] R.H. Davis, J.A. Schonberg, J.M. Rallison, The lubrication force between two viscous drops, *Phys. Fluids A*, 1 (1989) 77–81.